PHYSICAL REVIEW E **69**, 035401(R) (2004)

Effect of self-injection on ultraintense laser wake-field acceleration

A. Zhidkov,[1] J. Koga,[2] K. Kinoshita,[1] and M. Uesaka[1]
[1]*Nuclear Engineering Research Laboratory, Graduate School of Engineering, The University of Tokyo, 22-2 Shirane-shirakata, Tokai, Naka, Ibaraki 319-1188, Japan*
[2]*Advanced Photon Research Center, Japan Atomic Energy Research Institute, 8-1 Umemidai, Kizu-chou, Souraku-gun, Kyoto 619-0215, Japan*

(Received 11 February 2002; revised manuscript received 24 January 2003; published 31 March 2004)

The self-injection of plasma electrons which have been accelerated to relativistic energies by a laser pulse moving with a group velocity less than the speed of light with $I\lambda^2 > 5\times 10^{19}$ W μm^2/cm^2 is found via particle-in-cell simulation to be efficient for laser wake-field acceleration. When the matching condition $a_0 \geqslant (2^{1/4}\omega/\omega_{\rm pl})^{2/3}$ is met, the self-injection, along with wave breaking, dominates monoenergetic electron acceleration yielding up to 100 MeV energies by a 100 TW, 20 fs laser pulse. In contrast to the injection due to wave-breaking processes, self-injection allows suppression of production of a Maxwell distribution of accelerated particles and the extraction of a beam-quality bunch of energetic electrons.

DOI: 10.1103/PhysRevE.69.0354XX PACS number(s): 52.38.Kd, 41.75.Jv, 52.65.Rr

The laser wake-field acceleration (LWFA) of electrons in underdense plasmas [1] has been the subject of intense study for many years. This process is expected to be the basis for efficient and compact electron accelerators [2–4]. Recently, the necessity of short-pulse ($\sim$10 fs) electron beams with total charge large enough for probe analysis [5] raises interest in laser wake-field acceleration as a promising source for such beams.

For relativistically intense laser pulses, $I\lambda^2 > 10^{19}$ W μm^2/cm^2, electron acceleration by the wake field in relatively low density plasmas is not well understood. Several recent experimental [3,4,6] and numerical [7–10] works have concentrated on high density plasmas with strong wave breaking though new phenomenon in this regime, such as cavity formation [11] and corresponding effects, seem to appear. In addition to the common wake field and a longitudinal plasma wave with group velocity $v_{\rm gr}=0$, a relativistically intense laser pulse can produce a wave that moves with nonzero group velocity in the wake. This wave generated by temporally trapped electrons does not brake and may serve as a mechanism for a more efficient production of short electron bunches than the usual wake field due to a longer acceleration length.

It is well known that electron injection is a crucial part of wake-field acceleration. In the usual injection schemes for LWFA, in coincidence with the laser pulse a high quality electron beam from a conventional linac is injected and then further accelerated by the wake field [2]. Other schemes inject electrons from the background plasma via the interaction of additional injected laser pulses [4] or by wave breaking [3,6,8]. The latter is the simplest way using an intense laser pulse to generate energetic electrons and wakes. However, the wave breaking is initially a stochastic process that provokes rapid randomization in energy of accelerated electrons. This makes this kind of injection sometimes inefficient and usually very sensitive to plasma parameter changes. In the present paper we discuss an alternative mechanism of electron injection originating from the relativistic character of the laser-plasma interaction.

Along with the common wake field, a relativistically intense laser pulse moving in an underdense plasma with group velocity less than the light speed generates an additional electrostatic wave, which has a group velocity close to the group velocity of the laser pulse according to linear theory. This wave originates from temporally trapped electrons which have been directly accelerated by the laser pulse forming a bunch at the front of the laser pulse. This bunching of electrons creates a potential difference, potential cavity [11], behind the laser pulse due to the evacuation of electrons. The number of electrons in this bunch is limited. As the number of electrons in the bunch increases eventually there will be a point when the repulsive force of the bunch exceeds the ponderomotive one. Once this occurs additional background electrons are repelled by the bunch, but are accelerated to a maximal energy equal to the potential difference of the cavity and, having velocities equal to or larger than the group velocity of the laser pulse (if a proper matching condition occurs), can be efficiently injected for further acceleration in the same cavity. However, this injection, which can be considered as a self-injection, contends with injection from wave breaking. At low plasma density the self-injection produces efficient acceleration with a low energy spread while at high density, wave breaking dominates, producing a Maxwellian distribution of energetic electrons with an effective temperature.

Propagating in an underdense plasma with group velocity v_g, an intense laser pulse can accelerate plasma electrons longitudinally up to the energy $\varepsilon_{e\,\max}=mc^2a_0^2/2$ (for transverse acceleration the maximal energy cannot exceed mc^2a_0 [12]), where $a_0=eE/mc\omega$ with E the laser electric field and ω the laser frequency. If the velocity of such electrons exceeds the group velocity of the linearly polarized laser pulse [13], these electrons can be trapped and move with the pulse, forming an electrostatic wave. The matching condition can be written in the following form (see also [14]):

$$\gamma_{e\,\max}=a_0^2/2=\gamma_g=1/\sqrt{1-v_g^2/c^2}\approx\omega(\tilde{\gamma}_e/2)^{1/2}/\omega_{\rm pl} \quad (1)$$

where $\omega_{\rm pl}$ is the plasma frequency and $\tilde{\gamma}_e\sim\sqrt{1+a_0^2/2}$ is the electron quiver energy. [For a laser intensity $I=10^{20}$ W/cm^2, $\lambda=1$ μm: $a_0=5.3$, $N_{e\,\rm match}\sim 5\times 10^{18}$ cm^{-3}; for $a_0 \gg 1$ the matching occurs for a_0

 ©2004 The American Physical Society

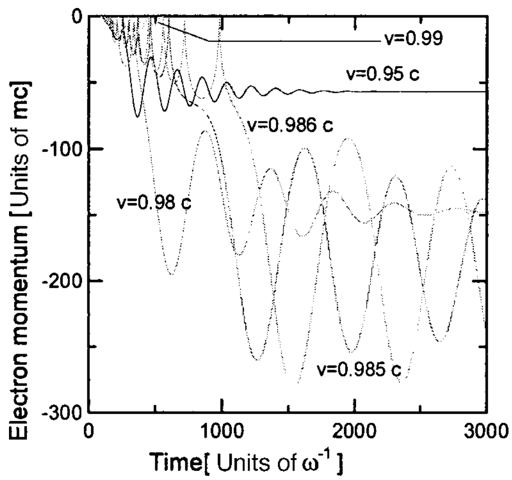

FIG. 1. The temporal evolution of the electron momentum in an electromagnetic field propagating in the $-x$ direction with group velocity ν_g.

$\geqslant(2^{1/4}\omega/\omega_{\rm pl})^{2/3}$.] To verify this, one can consider a simple model assuming that an initially stationary electron moves in an electromagnetic plane wave with a group velocity less than the speed of light, $a(x,t)=a_0\cos(t+x/\nu_g)\exp[-(x/\nu_g+t)^2/\tau^2]$ where τ is the pulse duration. Results of a simple numerical solution of the equation of motion with the fields determined above and the group velocity as a parameter are shown in Fig. 1 for a laser pulse with $a_0=8$ and pulse duration 20 fs. If the group velocity of the wave is close to the speed of light, the electron acquires the maximal energy $\gamma=a_0^2/2$ and, then, loses it after falling behind the pulse. As seen in Fig. 1 when the matching condition is met, the electron spends the longest time in the laser wave and, therefore, gets the largest acceleration.

The potential difference, $\Delta\phi$, produced by electrons directly accelerated by the laser field at the front of the pulse cannot exceed the ponderomotive potential $mc^2a_0^2/2$. As a result we get

$$e|\Delta\phi|\approx 2\pi ze^2N_id^2=mc^2a_0^2/2, \tag{2}$$

where z is the ion charge, N_i is the ion density, and d is the length of the cavity behind the laser pulse [15]. From Eq. (2) one can easily estimate the maximal charge of trapped electrons, $Q=eN_e\lambda_pa_0S/2\pi$, with λ_p the wake-field wavelength and S the square of the laser focus spot. Setting $S=5\times10^{-6}$ cm^2, we get $Q\sim10$ nC per 1 J of the laser energy for $N_e=10^{19}$ cm^{-3}. The length of the cavity behind the laser pulse is $d=\lambda_pa_0/2\pi$. At this distance behind the laser pulse the repelled electrons acquire energy $\varepsilon=|\Delta\phi|$ and, moving with the group velocity, are further accelerated in the cavity. For monoenergetic acceleration, d must exceed the pulse length $c\tau$, where τ is the pulse duration. Otherwise, the electrons interact with the laser field which would accelerate or decelerate the electrons based on their position in the field. The maximal energy finally acquired by such an electron is $E_{\rm max}=(a_0/2\pi)E_{\rm max}^{\rm WF}$, where $E_{\rm max}^{\rm WF}$ is the corresponding maximal energy in acceleration by a longitudinal plasma wave [4].

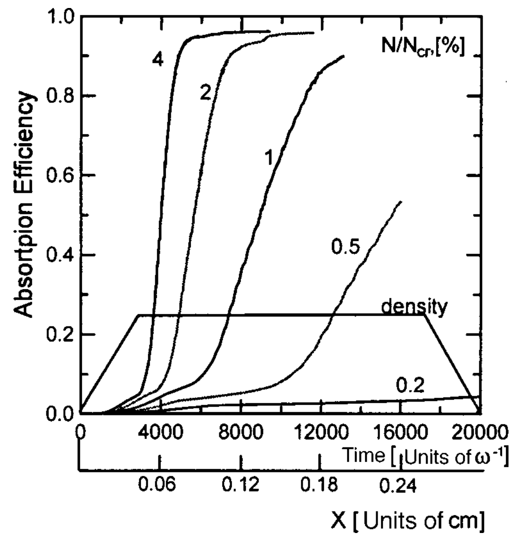

FIG. 2. The temporal evolution of the absorption rate of the laser pulse with intensity $I=10^{20}$ W/cm^2 for different plasma densities where the numbers beside the solid lines indicate the percentage of the critical density.

To study details of the self-injection mechanism, we apply a fully relativistic one-dimensional (1D) particle-in-cell (PIC), which corresponds to a large focus spot $d>30\ \mu$m and a more realistic 2D PIC (for s- and p-polarized laser pulses, $\lambda=1\ \mu$m) simulation with the "moving window" technique [16,17] with movable He ions. The plasma length is set to 3 mm, with a density gradient of length 0.5 mm on either edge (see Fig. 2). In the 2D simulation, we use nine particles per cell in a $160\ \mu\text{m}\times120\ \mu$m ($2800\times2048$ cells) window which moves at the speed of light. A full width at half maximum (FWHM) laser pulse with the duration of 20 fs and intensity of $I=10^{20-21}$ W/cm^2 [18] is focused on a 17 μm spot which corresponds to a Rayleigh length of 720 μm. The difference between the absorbed laser energy and the total plasma energy is controlled to be less than 1%. The numerical error in the group velocity is smaller than the velocity deviation from the speed of light. No plasma ionization is included. The electron density is varied from 2×10^{18} to 5×10^{19} cm^{-3} for the laser intensity to exceed the critical power for self-focusing $P_{\rm cr}=17(\omega/\omega_{\rm pl})^2$ GW since the length of the laser pulse is longer than the critical λ_p/a_0 [4].

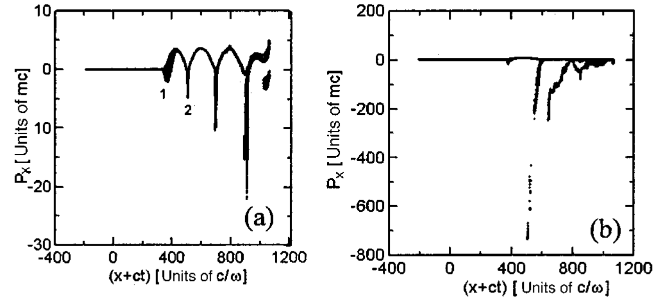

FIG. 3. The spatial distribution of electron longitudinal momentum P_x at (a) $\omega t=4000$, (b) $\omega t=10\,000$ at the laser intensity $I=10^{20}$ W/cm^2 and plasma density $N_e=5\times10^{18}$ cm^{-3}.

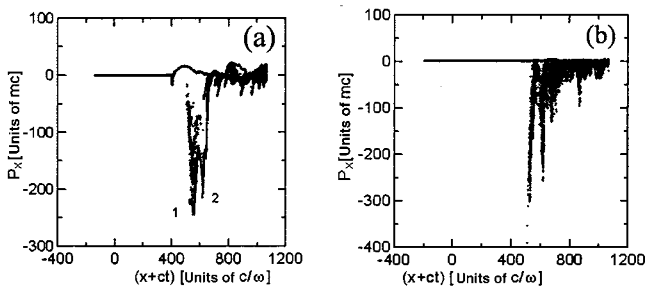

FIG. 4. The spatial distribution of electron longitudinal momentum P_x at the laser intensity $I=10^{20}$ W/cm^2 and $\omega t=6000$; plasma density (a) $N_e=2\times10^{19}$ cm^{-3} and (b) $N_e=5\times10^{19}$ cm^{-3}.

The absorption rate of the laser pulse with the intensity $I=10^{20}$ W/cm^2 is shown in Fig. 2 for different plasma densities. The absorption rate increases nonlinearly with the plasma density, $\sim N_e^{3/2}$, though energy losses for the wakefield excitation and electron acceleration by the potential difference given in Eq. (2) linearly depends on the plasma density. This nonlinear dependence could be explained by the frequency downshift; this absorption mechanism is given in Ref. [10]. For the considered pulse duration $t\omega_{\rm pl}\gg(2)^{3/2}|\mathbf{a}_0|^{-1}$ and the depletion time is $T=(8/3\sqrt{2})|a_0|^{-1}\omega_0^2/\omega_{\rm pl}^3\propto N_e^{-3/2}$. However, the numerical depletion time in Fig. 2 is ten times longer than the analytical prediction for all plasma densities. We attribute this delay to the time needed for the formation of a second electron bunch (explained below), which is responsible for the frequency downshift.

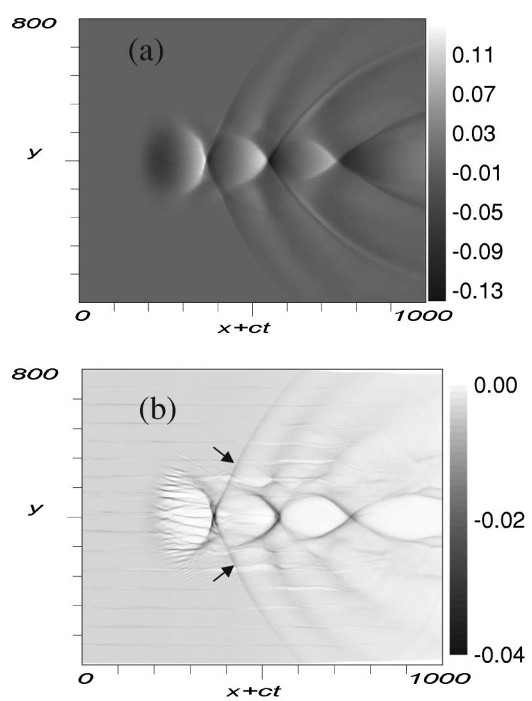

FIG. 5. The spatial distribution of the (a) normalized density of electrons with energy over 4 MeV where the circle indicates the position of the laser (ponderomotively scattered electrons are indicated by the arrows) and (b) the normalized x component of the plasma electrostatic field in a gas jet of density, $N_e=10^{19}$ cm^{-3}, at $\omega t=4000$ for $I=10^{20}$ W/cm^2.

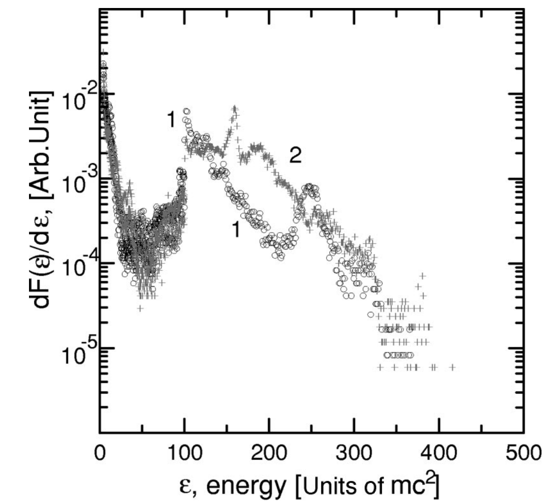

FIG. 6. Electron energy distribution in a 2D simulation; (1) $\omega t=6000$ and (2) $\omega t=12\,000$ at the plasma density $N_e=10^{19}$ cm^{-3}.

The spatial distribution of the longitudinal momentum of electrons in the plasma at different times is shown in Fig. 3 and Fig. 4. For the lower density plasma, Fig. 3, the mechanism of electron injection is totally different from that in the higher density plasma, Fig. 4, where the wave-breaking process is dominant. As seen in Fig. 3 for lower density plasmas, when the maximum charge that can be sustained by the laser pulse is reached, a second electrostatic bunch is produced (indicated by 2); electrons repelled from the first bunch (indicated by 1) and accelerated by the potential difference form it. Then, electrons from the second bunch are further accelerated forming almost monoenergetic bunches at $\varepsilon\sim130$ MeV, their maximal energy is $\varepsilon\sim400$ MeV. In higher density plasmas, the wave-breaking process becomes important as presented in Fig. 4. One can see two bunches originating from different processes: the first bunch (indicated by 1) is due to self-injection and the second (indicated by 2) is due to the wave-breaking injection [8]. According to particle trajectories, the first bunch is formed by electrons which are initially accelerated by the laser pulse and, after passing through the cavity potential produced by ions, get trapped. With the density increase, the energy distribution of accelerated electrons approaches a Maxwellian distribution in the second, ‘‘wave-breaking,’’ bunch formed by electrons coming from behind the cavity. At the minimal laser intensity, $I\sim5\times10^{19}$ W/cm^2, the self-injection appears in a narrow density range. This density range increases with intensity and is $(0.5\text{–}2)\times10^{19}$ cm^{-3} at $I=10^{20}$ W/cm^2.

Results of a 2D simulation for an s-polarized pulse are shown in Fig. 5. One can see a clear cavity structure in the electron density with the trapped electrons in the front of the laser pulse in Fig. 5(a), where the circle indicates the laser position after the pulse has propagated 0.5 mm in the plasma; however, there is no wave breaking of the plasma wave according to Fig. 5(b) which shows the x component of the electrostatic field. The transverse size of the first bunch in the rear of the first cavity is about 10 μm. The density of electron bunches which have formed behind the laser pulse decreases with distance from the laser pulse; traces of electrons expelled on either side of the pulse (indicated by arrows) are produced by nonlinear ponderomotive scattering [12]. The energy distribution of electrons in the bunch behind the pulse after propagating 1 mm and 2 mm in the plasma are shown in Fig. 6. Both distributions have a peak (indicated by arrows) that corresponds to electrons accelerated after the self-injection. The energy in the peak is lower than that obtained in 1D simulations. We attribute this to the dimensional effect on the potential difference. The energy spread (e^{-1} from the maximal density) is 5% in both cases although the energy spread in the pedestal increases considerably. Formal calculation of the longitudinal emittance of the bunch gives 0.1π mm mrad with a total charge of $Q\sim 200$ pC. Simulation for a p-polarized pulse gives qualitatively similar results.

In conclusion, we have observed the effect of self-injection on electron wake-field acceleration by an ultrarelativistic laser pulse via a fully relativistic particle-in-cell simulation. We have demonstrated that two electron bunches can be formed in a plasma by an intense laser pulse; the first consists of electrons at the front of the laser directly accelerated by the laser pulse. The second is generated by electrons expelled from the first bunch and then accelerated by the potential difference in the wake to a velocity equal to the group velocity of the laser pulse. Electrons, which form the second bunch, are further accelerated by the same field. Due to the regular character of this mechanism, in contrast to the injection due to the stochastic wave breaking, a bunch of accelerated electrons with a total charge ~ 200 pC per 1 J of laser energy has a relatively small energy spread; its longitudinal emittance is about 0.1π mm mrad. This process also dominates the nonlinear growth of the absorption rate with plasma density.

This work was partially supported by National Institute of Radiological Sciences, Japan.

[1] T. Tajima and J. Dawson, Phys. Rev. Lett. **43**, 267 (1979).
[2] K. Nakajima *et al.*, Phys. Rev. Lett. **74**, 4428 (1995); F. Amiranoff *et al.*, *ibid.* **81**, 995 (1998); F. Dorchies *et al.*, Phys. Plasmas **6**, 2903 (1999).
[3] D. Umstadter *et al.*, Science **273**, 472 (1996); Phys. Rev. Lett. **76**, 2073 (1996).
[4] E. Esarey *et al.*, Phys. Rev. Lett. **79**, 2682 (1997); IEEE Trans. Plasma Sci. **24**, 252 (1996).
[5] M. Uesaka *et al.*, Phys. Rev. E **50**, 3068 (1994); Radiat. Phys. Chem. **60**, 303 (2001); Nucl. Instrum. Methods Phys. Res. A **455**, 148 (2000).
[6] V. Malka *et al.*, Phys. Plasmas **8**, 2605 (2001); Science **298**, 1600 (2002).
[7] S. V. Bulanov, V. I. Kirsanov, and A. S. Sakharov, JETP Lett. **53**, 565 (1991).
[8] S. Bulanov, N. Naumova, F. Pegoraro, and J. Sakai, Phys. Rev. E **58**, R5257 (1998).
[9] Y. Ueshima *et al.*, Nucl. Instrum. Methods Phys. Res. A **445**, 130 (2000).
[10] S. V. Bulanov *et al.*, Phys. Fluids B **4**, 1935 (1992).
[11] A. Pukhov and J. Meyer-ter-Vehn, Appl. Phys. B: Lasers Opt. **74**, 355 (2002).
[12] F. V. Hartemann *et al.*, Phys. Rev. E **51**, 4833 (1995).
[13] C. D. Decker and W. B. Mori, Phys. Rev. E **51**, 1364 (1995).
[14] C. J. McKinstrie and E. A. Startsev, Phys. Rev. E **56**, 2130 (1997).
[15] We assume that the length, d_e, of the electron cloud generated at the front of the pulse is such that $d_e \ll d$.
[16] C. K. Birdsall and A. B. Langdon, *Plasma Physics via Computer Simulation* (Adam Hilger, Bristol, 1992).
[17] R. G. Hemker *et al.*, Phys. Rev. ST Accel. Beams **5**, 041301 (2002).
[18] The laser parameters are chosen close to those of the JAERI laser with the maximal power 0.85 PW; see M. Aoyama *et al.*, Opt. Lett. **28**, 1594 (2003).